

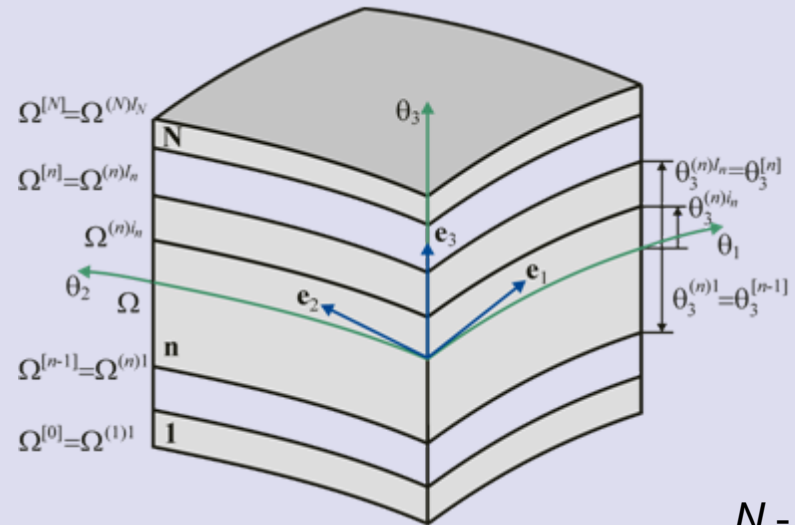
A New Approach to 3D Exact Thermoelastic Analysis of Functionally Graded Laminated Plates and Shells

G.M. Kulikov and S.V. Plotnikova

Speaker: Gennady Kulikov

Department of Applied Mathematics & Mechanics

Description of Temperature Field



$\Omega^{(n)1}, \Omega^{(n)2}, \dots, \Omega^{(n)I_n}$ - sampling surfaces (SaS)

$\theta_3^{(n)I_n}$ - transverse coordinates of SaS

$\theta_3^{[n-1]}, \theta_3^{[n]}$ - transverse coordinates of interfaces

$$\theta_3^{(n)1} = \theta_3^{[n-1]}, \quad \theta_3^{(n)I_n} = \theta_3^{[n]} \quad (1)$$

$$\theta_3^{(n)m_n} = \frac{1}{2}(\theta_3^{[n-1]} + \theta_3^{[n]}) - \frac{1}{2}h_n \cos\left(\pi \frac{2m_n - 3}{2(I_n - 2)}\right)$$

N - number of layers; I_n - number of SaS of the n th layer

$n = 1, 2, \dots, N; i_n = 1, 2, \dots, I_n; m_n = 2, 3, \dots, I_n - 1$

Temperature Gradient Γ in Orthonormal Basis

$$\Gamma_\alpha = \frac{1}{A_\alpha c_\alpha} T_{,\alpha}, \quad \Gamma_3 = T_{,3} \quad (2)$$

$T(\theta_1, \theta_2, \theta_3)$ – temperature; $c_\alpha = 1 + k_\alpha \theta_3$ – components of shifter tensor at SaS

$A_\alpha(\theta_1, \theta_2), k_\alpha(\theta_1, \theta_2)$ – Lamé coefficients and principal curvatures of midsurface Ω

Temperature Distribution in Thickness Direction

$$T^{(n)} = \sum_{i_n} L^{(n)i_n} T^{(n)i_n}, \quad T^{(n)i_n} = T\left(\theta_3^{(n)i_n}\right), \quad \theta_3^{[n-1]} \leq \theta_3 \leq \theta_3^{[n]} \quad (3)$$

$$L^{(n)i_n} = \prod_{j_n \neq i_n} \frac{\theta_3 - \theta_3^{(n)j_n}}{\theta_3^{(n)i_n} - \theta_3^{(n)j_n}} \quad (4)$$

$T^{(n)i_n}(\theta_1, \theta_2)$ – temperatures of SaS; $L^{(n)i_n}(\theta_3)$ – Lagrange polynomials of degree I_n - 1

Temperature Gradient Distribution in Thickness Direction

$$\Gamma_i^{(n)} = \sum_{i_n} L^{(n)i_n} \Gamma_i^{(n)i_n}, \quad \Gamma_i^{(n)i_n} = \Gamma_i(\theta_3^{(n)i_n}), \quad \theta_3^{[n-1]} \leq \theta_3 \leq \theta_3^{[n]} \quad (5)$$

$\Gamma_i^{(n)i_n}(\theta_1, \theta_2)$ – temperature gradient at SaS

Relations between Temperature Gradient and Temperature

$$\Gamma_{\alpha}^{(n)i_n} = \frac{1}{A_{\alpha} c_{\alpha}^{(n)i_n}} T_{,\alpha}^{(n)i_n} \quad (6)$$

$$\Gamma_3^{(n)i_n} = \sum_{j_n} M^{(n)j_n}(\theta_3^{(n)i_n}) T^{(n)j_n} \quad (7)$$

$$c_{\alpha}^{(n)i_n} = c_{\alpha}(\theta_3^{(n)i_n}) = 1 + k_{\alpha} \theta_3^{(n)i_n}$$

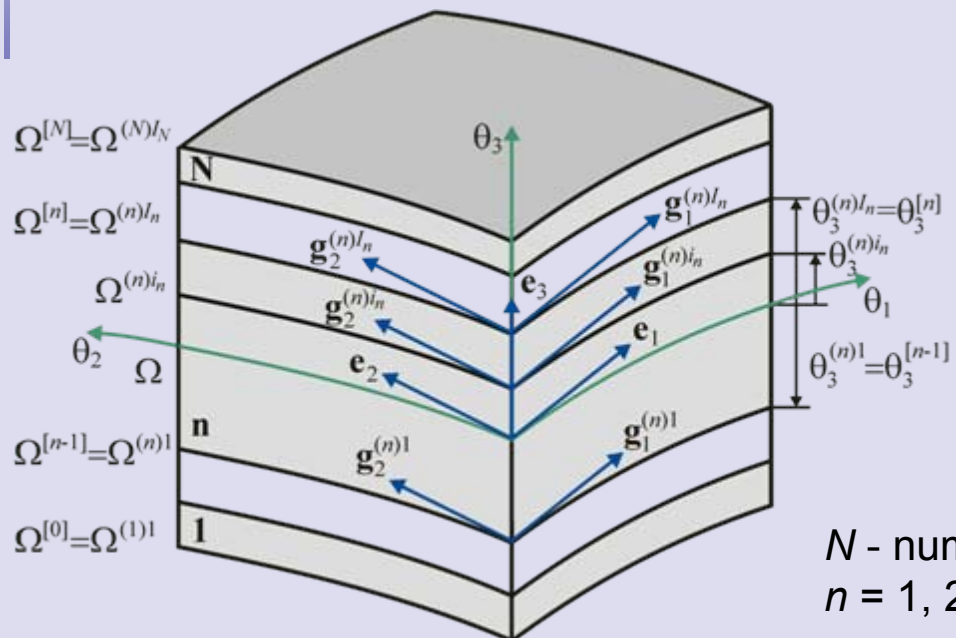
$c_{\alpha}^{(n)i_n}(\theta_1, \theta_2)$ – components of shifter tensor at SaS

Derivatives of Lagrange Polynomials at SaS

$$M^{(n)j_n}(\theta_3^{(n)i_n}) = \frac{1}{\theta_3^{(n)j_n} - \theta_3^{(n)i_n}} \prod_{k_n \neq i_n, j_n} \frac{\theta_3^{(n)i_n} - \theta_3^{(n)k_n}}{\theta_3^{(n)j_n} - \theta_3^{(n)k_n}} \text{ for } j_n \neq i_n \quad (8)$$

$$M^{(n)i_n}(\theta_3^{(n)i_n}) = - \sum_{j_n \neq i_n} M^{(n)j_n}(\theta_3^{(n)i_n}), \quad M^{(n)j_n} = L_{,3}^{(n)j_n}$$

Kinematic Description of Undeformed Shell



$\Omega^{(n)1}, \Omega^{(n)2}, \dots, \Omega^{(n)I_n}$ - sampling surfaces (SaS)

$\theta_3^{(n)i_n}$ - transverse coordinates of SaS

$\theta_3^{[n-1]}, \theta_3^{[n]}$ - transverse coordinates of interfaces

$$\theta_3^{(n)1} = \theta_3^{[n-1]}, \quad \theta_3^{(n)I_n} = \theta_3^{[n]} \quad (9)$$

$$\theta_3^{(n)m_n} = \frac{1}{2}(\theta_3^{[n-1]} + \theta_3^{[n]}) - \frac{1}{2}h_n \cos\left(\pi \frac{2m_n - 3}{2(I_n - 2)}\right)$$

N - number of layers; I_n - number of SaS of the n th layer
 $n = 1, 2, \dots, N$; $i_n = 1, 2, \dots, I_n$; $m_n = 2, 3, \dots, I_n - 1$

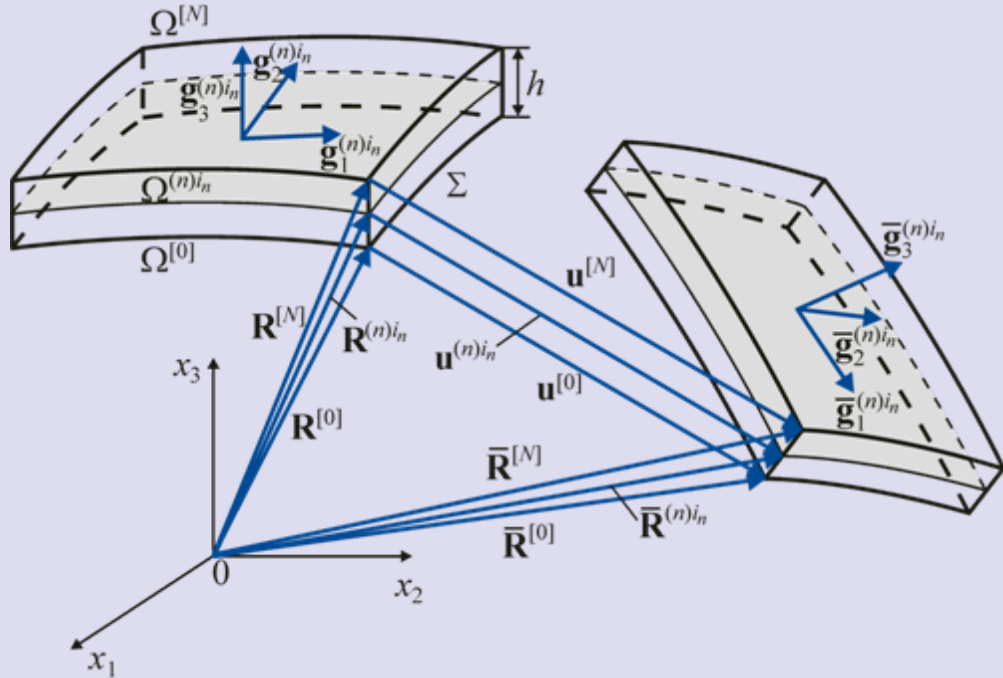
Position Vectors and Base Vectors of SaS

$$\mathbf{R}^{(n)i_n} = \mathbf{r} + \theta_3^{(n)i_n} \mathbf{e}_3 \quad (10)$$

$$\mathbf{g}_\alpha^{(n)i_n} = \mathbf{R}_{,\alpha}^{(n)i_n} = A_\alpha C_\alpha^{(n)i_n} \mathbf{e}_\alpha, \quad \mathbf{g}_3^{(n)i_n} = \mathbf{e}_3 \quad (11)$$

$\mathbf{r}(\theta_1, \theta_2)$ – position vector of midsurface Ω ; $\mathbf{e}_i(\theta_1, \theta_2)$ – orthonormal base vectors of midsurface Ω

Kinematic Description of Deformed Shell



Position Vectors of Deformed SaS

$$\bar{\mathbf{R}}^{(n)i_n} = \mathbf{R}^{(n)i_n} + \mathbf{u}^{(n)i_n} \quad (12)$$

$$\mathbf{u}^{(n)i_n} = \mathbf{u}(\theta_3^{(n)i_n}) \quad (13)$$

$\mathbf{u}(\theta_1, \theta_2, \theta_3)$ – displacement vector

$\mathbf{u}^{(n)i_n}(\theta_1, \theta_2)$ – displacement vectors of SaS

Base Vectors of Deformed SaS

$$\mathbf{g}_\alpha^{(n)i_n} = \bar{\mathbf{R}}_{,\alpha}^{(n)i_n} = \mathbf{g}_\alpha^{(n)i_n} + \mathbf{u}_{,\alpha}^{(n)i_n}, \quad \mathbf{g}_3^{(n)i_n} = \mathbf{e}_3 + \beta^{(n)i_n}, \quad \beta^{(n)i_n} = \mathbf{u}_{,3}(\theta_3^{(n)i_n}) \quad (14)$$

$\beta^{(n)i_n}(\theta_1, \theta_2)$ – values of derivative of displacement vector at SaS

Green-Lagrange Strain Tensor at SaS

$$2\varepsilon_{ij}^{(n)i_n} = \frac{1}{A_i A_j c_i^{(n)i_n} c_j^{(n)i_n}} (\bar{\mathbf{g}}_i^{(n)i_n} \cdot \bar{\mathbf{g}}_j^{(n)i_n} - \mathbf{g}_i^{(n)i_n} \cdot \mathbf{g}_j^{(n)i_n}) \quad (15)$$

Linearized Strain Tensor at SaS

$$2\varepsilon_{\alpha\beta}^{(n)i_n} = \frac{1}{A_\alpha c_\alpha^{(n)i_n}} \mathbf{u}_{,\alpha}^{(n)i_n} \cdot \mathbf{e}_\beta + \frac{1}{A_\beta c_\beta^{(n)i_n}} \mathbf{u}_{,\beta}^{(n)i_n} \cdot \mathbf{e}_\alpha \quad (16)$$

$$2\varepsilon_{\alpha 3}^{(n)i_n} = \beta^{(n)i_n} \cdot \mathbf{e}_\alpha + \frac{1}{A_\alpha c_\alpha^{(n)i_n}} \mathbf{u}_{,\alpha}^{(n)i_n} \cdot \mathbf{e}_3, \quad \varepsilon_{33}^{(n)i_n} = \beta^{(n)i_n} \cdot \mathbf{e}_3$$

Displacement Vectors of SaS in Orthonormal Basis

$$\mathbf{u}^{(n)i_n} = u_i^{(n)i_n} \mathbf{e}_i, \quad \beta^{(n)i_n} = \beta_i^{(n)i_n} \mathbf{e}_i \quad (17)$$

Derivatives of Displacement Vectors in Orthonormal Basis

$$\frac{1}{A_\alpha} \mathbf{u}_{,\alpha}^{(n)i_n} = \lambda_{i\alpha}^{(n)i_n} \mathbf{e}_i \quad (18)$$

Strain Parameters of SaS

$$\begin{aligned} \lambda_{\alpha\alpha}^{(n)i_n} &= \frac{1}{A_\alpha} u_{\alpha,\alpha}^{(n)i_n} + B_\alpha u_\beta^{(n)i_n} + k_\alpha u_3^{(n)i_n}, & \lambda_{\beta\alpha}^{(n)i_n} &= \frac{1}{A_\alpha} u_{\beta,\alpha}^{(n)i_n} - B_\alpha u_\alpha^{(n)i_n} \quad (\beta \neq \alpha) \\ \lambda_{3\alpha}^{(n)i_n} &= \frac{1}{A_\alpha} u_{3,\alpha}^{(n)i_n} - k_\alpha u_\alpha^{(n)i_n}, & B_\alpha &= \frac{1}{A_\alpha A_\beta} A_{\alpha,\beta} \quad (\beta \neq \alpha) \end{aligned} \quad (19)$$

Linearized Strains of SaS

$$2\varepsilon_{\alpha\beta}^{(n)i_n} = \frac{1}{c_\beta^{(n)i_n}} \lambda_{\alpha\beta}^{(n)i_n} + \frac{1}{c_\alpha^{(n)i_n}} \lambda_{\beta\alpha}^{(n)i_n} \quad (20)$$

$$2\varepsilon_{\alpha 3}^{(n)i_n} = \beta_\alpha^{(n)i_n} + \frac{1}{c_\alpha^{(n)i_n}} \lambda_{3\alpha}^{(n)i_n}, \quad \varepsilon_{33}^{(n)i_n} = \beta_3^{(n)i_n}$$

Remark. Strains (20) exactly represent all rigid-body shell motions in any convected curvilinear coordinate system. It can be proved through results of Kulikov and Carrera (2008)

Displacement Distribution in Thickness Direction

$$u_i^{(n)} = \sum_{i_n} L^{(n)i_n} u_i^{(n)i_n}, \quad \theta_3^{[n-1]} \leq \theta_3 \leq \theta_3^{[n]} \quad (21)$$

Strain Distribution in Thickness Direction

$$\varepsilon_{ij}^{(n)} = \sum_{i_n} L^{(n)i_n} \varepsilon_{ij}^{(n)i_n}, \quad \theta_3^{[n-1]} \leq \theta_3 \leq \theta_3^{[n]} \quad (22)$$

Presentation for Derivative of Displacement Vector

$$\beta_i^{(n)i_n} = \sum_{j_n} M^{(n)j_n} (\theta_3^{(n)i_n}) u_i^{(n)j_n}, \quad M^{(n)j_n} = L_{,3}^{(n)j_n} \quad (23)$$

Variational Formulation of Thermal Problem

$$\delta J = 0 \quad (24)$$

$$J = \frac{1}{2} \iint_{\Omega} \sum_n \int_{\theta_3^{[n-1]}}^{\theta_3^{[n]}} q_i^{(n)} \Gamma_i^{(n)} A_1 A_2 c_1 c_2 d\theta_1 d\theta_2 d\theta_3 - \iint_{\Omega} T Q_n d\Omega \quad (25)$$

$q_i^{(n)}$ – heat flux of the n th layer; Q_n – specified heat flux

Heat Flux Resultants

$$R_i^{(n)i_n} = \int_{\theta_3^{[n-1]}}^{\theta_3^{[n]}} q_i^{(n)} L^{(n)i_n} c_1 c_2 d\theta_3 \quad (26)$$

Basic Functional of Heat Conduction Theory

$$J = \frac{1}{2} \iint_{\Omega} \sum_n \sum_{i_n} R_i^{(n)i_n} \Gamma_i^{(n)i_n} A_1 A_2 d\theta_1 d\theta_2 - \iint_{\Omega} T Q_n d\Omega \quad (27)$$

Fourier Heat Conduction Equations

$$q_i^{(n)} = -k_{ij}^{(n)} \Gamma_j^{(n)}, \quad \theta_3^{[n-1]} \leq \theta_3 \leq \theta_3^{[n]} \quad (28)$$

$k_{ij}^{(n)}$ – thermal conductivity tensor of the n th layer

Distribution of Thermal Conductivities in Thickness Direction

$$k_{ij}^{(n)} = \sum_{i_n} L^{(n)i_n} k_{ij}^{(n)i_n} \quad (29)$$

Heat Flux Resultants

$$R_i^{(n)i_n} = - \sum_{j_n, k_n} \Lambda^{(n)i_n j_n k_n} k_{ij}^{(n)j_n} \Gamma_j^{(n)k_n} \quad (30)$$

$$\Lambda^{(n)i_n j_n k_n} = \int_{\theta_3^{[n-1]}}^{\theta_3^{[n]}} L^{(n)i_n} L^{(n)j_n} L^{(n)k_n} c_1 c_2 d\theta_3 \quad (31)$$

Variational Formulation of Thermoelastic Problem

Variational Equation

$$\delta\Pi = 0 \quad (32)$$

$$\Pi = \iint_{\Omega} \sum_n \int_{\theta_3^{[n-1]}}^{\theta_3^{[n]}} F^{(n)} A_1 A_2 c_1 c_2 d\theta_1 d\theta_2 d\theta_3 - W, \quad F^{(n)} = \frac{1}{2} (\sigma_{ij}^{(n)} \varepsilon_{ij}^{(n)} - \eta^{(n)} \Theta^{(n)}) \quad (33)$$

$F^{(n)}$ – free-energy density of the n th layer; $\sigma_{ij}^{(n)}$ – stress tensor of the n th layer

$\eta^{(n)}$ – entropy density of the n th layer; $\Theta^{(n)} = T^{(n)} - T_0$ – temperature rise of the n th layer

W – work done by external loads

Stress Resultants

$$H_{ij}^{(n)i_n} = \int_{\theta_3^{[n-1]}}^{\theta_3^{[n]}} \sigma_{ij}^{(n)} L^{(n)i_n} c_1 c_2 d\theta_3 \quad (34)$$

Entropy Resultants

$$S^{(n)i_n} = \int_{\theta_3^{[n-1]}}^{\theta_3^{[n]}} \eta^{(n)} L^{(n)i_n} c_1 c_2 d\theta_3 \quad (35)$$

Basic Functional of Thermoelasticity Theory

$$\Pi = \frac{1}{2} \iint_{\Omega} \sum_n \sum_{i_n} \left(H_{ij}^{(n)i_n} \varepsilon_{ij}^{(n)i_n} - S^{(n)i_n} \Theta^{(n)i_n} \right) A_1 A_2 d\theta_1 d\theta_2 - W \quad (36)$$

Constitutive Equations

$$\sigma_{ij}^{(n)} = C_{ijkl}^{(n)} \varepsilon_{kl}^{(n)} - \gamma_{ij}^{(n)} \Theta^{(n)}, \quad \theta_3^{[n-1]} \leq \theta_3 \leq \theta_3^{[n]} \quad (37)$$

$$\eta^{(n)} = \gamma_{kl}^{(n)} \varepsilon_{kl}^{(n)} + \chi^{(n)} \Theta^{(n)}, \quad \theta_3^{[n-1]} \leq \theta_3 \leq \theta_3^{[n]} \quad (38)$$

$C_{ijkl}^{(n)}$, $\gamma_{ij}^{(n)}$, $\chi^{(n)}$ – physical properties of the n th layer

Distribution of Material Constants in Thickness Direction

$$C_{ijkl}^{(n)i_n} = \sum_{i_n} L^{(n)i_n} C_{ijkl}^{(n)i_n}, \quad \gamma_{ij}^{(n)} = \sum_{i_n} L^{(n)i_n} \gamma_{ij}^{(n)i_n}, \quad \chi^{(n)} = \sum_{i_n} L^{(n)i_n} \chi^{(n)i_n} \quad (39)$$

$C_{ijkl}^{(n)i_n}$, $\gamma_{ij}^{(n)i_n}$, $\chi^{(n)i_n}$ – values of material constants on SaS of the n th layer

Presentations for Stress and Entropy Resultants

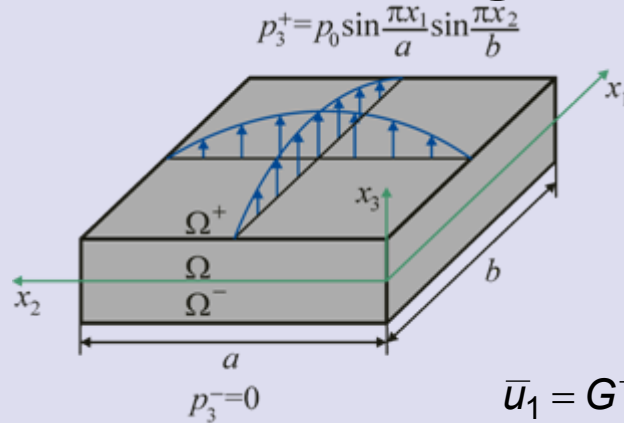
$$H_{ij}^{(n)i_n} = \sum_{j_n, k_n} \Lambda^{(n)i_n j_n k_n} \left(C_{ijkl}^{(n)j_n} \varepsilon_{kl}^{(n)k_n} - \gamma_{ij}^{(n)j_n} \Theta^{(n)k_n} \right) \quad (40)$$

$$S^{(n)i_n} = \sum_{j_n, k_n} \Lambda^{(n)i_n j_n k_n} \left(\gamma_{kl}^{(n)j_n} \varepsilon_{kl}^{(n)k_n} + \chi^{(n)j_n} \Theta^{(n)k_n} \right) \quad (41)$$

$$\Lambda^{(n)i_n j_n k_n} = \int_{\theta_3^{[n-1]}}^{\theta_3^{[n]}} L^{(n)i_n} L^{(n)j_n} L^{(n)k_n} c_1 c_2 d\theta_3 \quad (42)$$

Numerical Examples

1. FG Rectangular Plate under Mechanical Loading



Analytical solution

$$u_1^{(n)i_n} = \sum_{r,s} u_{1rs}^{(n)i_n} \cos \frac{r\pi x_1}{a} \sin \frac{s\pi x_2}{b}, \quad u_2^{(n)i_n} = \sum_{r,s} u_{2rs}^{(n)i_n} \sin \frac{r\pi x_1}{a} \cos \frac{s\pi x_2}{b}$$

$$u_3^{(n)i_n} = \sum_{r,s} u_{3rs}^{(n)i_n} \sin \frac{r\pi x_1}{a} \sin \frac{s\pi x_2}{b}$$

Dimensionless variables in crucial points

$$\bar{u}_1 = G^+ u_1(0, a/2, z) / hp_0, \quad \bar{u}_3 = G^+ u_3(a/2, a/2, z) / hp_0, \quad G^+ = E^+ / (2(1+\nu))$$

$$\bar{\sigma}_{11} = \sigma_{11}(a/2, a/2, z) / p_0, \quad \bar{\sigma}_{13} = \sigma_{13}(0, a/2, z) / p_0, \quad \bar{\sigma}_{33} = \sigma_{33}(a/2, a/2, z) / p_0$$

$$E = E^+ e^{\alpha(z-0.5)}, \quad \alpha = \ln(E^+ / E^-), \quad z = x_3 / h, \quad E^+ = 10^7 \text{ Pa}, \quad \nu = 0.3$$

Table 1. Results for a FG square plate for $a = b = 1 \text{ m}$, $a/h = 3$ and $\alpha = 0$

I_1	$-\bar{u}_1(0.5)$	$\bar{u}_3(0)$	$\bar{\sigma}_{11}(0.5)$	$\bar{\sigma}_{13}(0)$	$\bar{\sigma}_{33}(0)$
3	0.3986372494504680	1.278878243389591	1.999302146854837	0.4977436151168003	0.4752837277628003
7	0.4358933937131948	1.342554953466513	2.124032428288413	0.7022762666060094	0.4943950643281928
11	0.4358933942603120	1.342554689543095	2.124018410314048	0.7023022083223538	0.4944039935419638
15	0.4358933942603121	1.342554689542491	2.124018410193782	0.7023022084767580	0.4944039936052152
19	0.4358933942603120	1.342554689542491	2.124018410193780	0.7023022084767578	0.4944039936052150
Exact	0.4358933942603120	1.342554689542491	2.124018410193781	0.7023022084767578	0.4944039936052149

Exact results have been obtained by authors using Vlasov's closed-form solution (1957)

Table 2. Results for a FG square plate for $a = b = 1\text{ m}$, $a/h = 3$ and $\alpha = 0.1$

I_1	$-\bar{u}_1(0.5)$	$\bar{u}_3(0)$	$\bar{\sigma}_{11}(0.5)$	$\bar{\sigma}_{13}(0)$	$\bar{\sigma}_{33}(0)$
3	0.4158336502652652	1.347977241257294	2.073239906807475	0.4983226799021384	0.4596565434470269
7	0.4536977979133792	1.414636043682728	2.193265858989844	0.7020700339720654	0.4877173446168515
11	0.4536977984142576	1.414635771310962	2.193270258459039	0.7020957676355946	0.4877129579452970
15	0.4536977984142576	1.414635771310368	2.193270258650021	0.7020957677904856	0.4877129578319663
19	0.4536977984142575	1.414635771310368	2.193270258650021	0.7020957677904854	0.4877129578319657
Exact		1.41464			

Exact results have been obtained by Kashtalyan (2004)

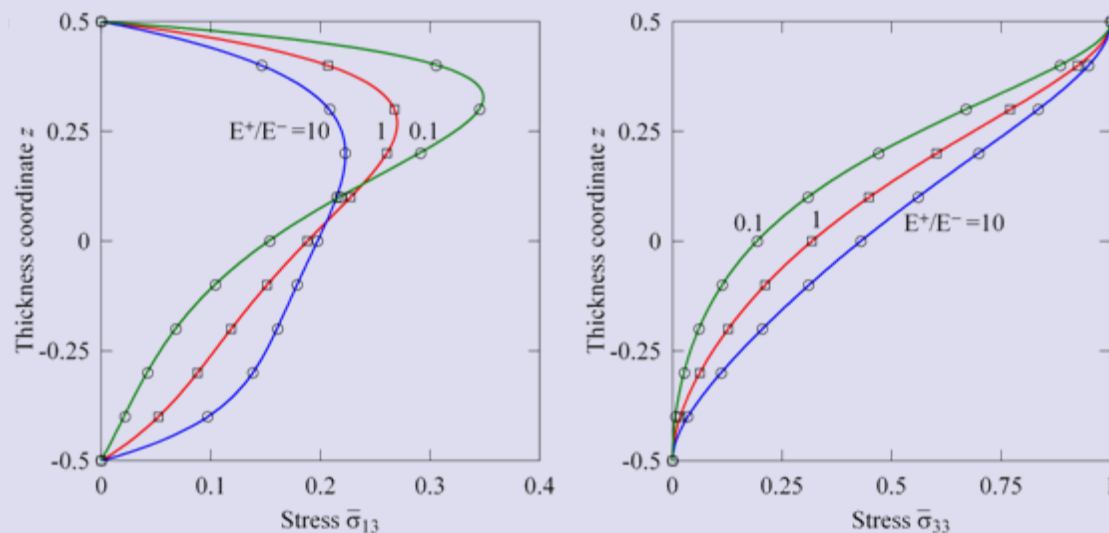
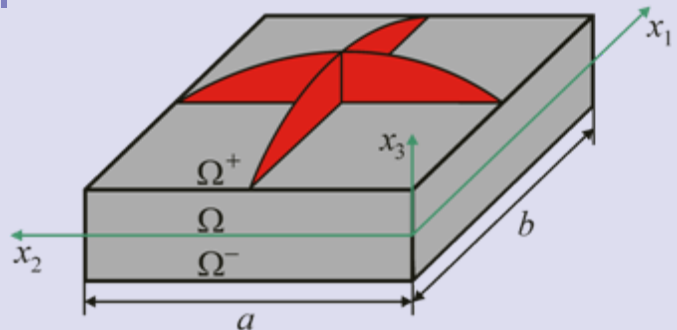


Figure 1. Through-thickness distributions of transverse stresses of FG plate with $a/h = 1$: present analysis (—) for $I_1 = 11$ and Vlasov's closed-form solution (\square), and Kashtalyan's closed-form solution (\circ)

2. Two-Phase FG Rectangular Plate under Temperature Loading

$$\Theta^+ = \Theta_0 \sin \frac{\pi x_1}{a} \sin \frac{\pi x_2}{b}, \quad \sigma_{13}^+ = \sigma_{23}^+ = \sigma_{33}^+ = 0$$



$$\Theta^- = 0, \quad \sigma_{13}^- = \sigma_{23}^- = \sigma_{33}^- = 0$$

Analytical solution

$$\Theta^{(n)i_n} = \sum_{r,s} \Theta_{rs}^{(n)i_n} \sin \frac{r\pi x_1}{a} \sin \frac{s\pi x_2}{b}, \quad u_1^{(n)i_n} = \sum_{r,s} u_{1rs}^{(n)i_n} \cos \frac{r\pi x_1}{a} \sin \frac{s\pi x_2}{b}$$

$$u_2^{(n)i_n} = \sum_{r,s} u_{2rs}^{(n)i_n} \sin \frac{r\pi x_1}{a} \cos \frac{s\pi x_2}{b}, \quad u_3^{(n)i_n} = \sum_{r,s} u_{3rs}^{(n)i_n} \sin \frac{r\pi x_1}{a} \sin \frac{s\pi x_2}{b}$$

Mori-Tanaka method is used for evaluating material properties of the Metal/Ceramic plate with
 $E_m = 7 \times 10^{10} \text{ Pa}$, $\nu_m = 0.3$, $\alpha_m = 23.4 \times 10^{-6} \text{ 1/K}$, $k_m = 233 \text{ W/mK}$, $\rho_m = 2707 \text{ Kg/m}^3$, $c_m = 896 \text{ J/KgK}$
 $E_c = 4.27 \times 10^{11} \text{ Pa}$, $\nu_c = 0.17$, $\alpha_c = 4.3 \times 10^{-6} \text{ 1/K}$, $k_c = 65 \text{ W/mK}$, $\rho_c = 3100 \text{ Kg/m}^3$, $c_c = 670 \text{ J/KgK}$

$$V_m = 1 - V_c, \quad V_c = V_c^- + (V_c^+ - V_c^-)(0.5 + z)^\gamma, \quad z = x_3 / h, \quad V_c^- = 0, \quad V_c^+ = 0.5, \quad \gamma = 2, \quad T_0 = 293 \text{ K}$$

where V_c^- , V_c^+ – volume fractions of the ceramic phase on bottom and top surfaces

Dimensionless variables in crucial points

$$\bar{\Theta} = \Theta(a/2, a/2, z)/\Theta_0, \quad \bar{q}_1 = -hq_1(0, a/2, z)/k_m\Theta_0$$

$$\bar{q}_3 = -hq_3(a/2, a/2, z)/k_m\Theta_0, \quad \bar{\eta} = \eta(a/2, a/2, z)/E_m\alpha_m^2\Theta_0$$

$$\bar{u}_1 = 10u_1(0, a/2, z)/a\alpha_m\Theta_0, \quad \bar{u}_3 = 100hu_3(a/2, a/2, z)/a^2\alpha_m\Theta_0$$

$$\bar{\sigma}_{11} = 10\sigma_{11}(a/2, a/2, z)/E_m\alpha_m\Theta_0, \quad \bar{\sigma}_{12} = 10\sigma_{12}(0, 0, z)/E_m\alpha_m\Theta_0$$

$$\bar{\sigma}_{13} = 100a\sigma_{13}(0, a/2, z)/hE_m\alpha_m\Theta_0, \quad \bar{\sigma}_{33} = 100a^2\sigma_{33}(a/2, a/2, z)/h^2E_m\alpha_m\Theta_0$$

Table 3. Results for a single-layer Metal/Ceramic square plate with $a = b = 1 \text{ m}$, $a/h = 5$

I_1	$\bar{u}_1(0.5)$	$\bar{u}_3(0.5)$	$\bar{\sigma}_{11}(0.5)$	$\bar{\sigma}_{12}(0.5)$	$\bar{\sigma}_{13}(0.25)$	$\bar{\sigma}_{33}(0)$	$\bar{\Theta}(0)$	$\bar{q}_1(0)$	$\bar{q}_3(-0.5)$	$\bar{\eta}(0)$
3	-1.2096	4.4213	-3.1907	-6.4775	4.3279	-266.58	0.39780	0.24994	0.59119	86.305
5	-1.2117	4.4198	-4.1612	-6.4890	5.0419	-6.3122	0.39379	0.24742	0.72392	85.605
7	-1.2101	4.4111	-4.1765	-6.4804	4.2085	-8.7894	0.39375	0.24740	0.73125	85.596
9	-1.2101	4.4111	-4.1764	-6.4804	4.2259	-8.6803	0.39375	0.24740	0.73158	85.596
11	-1.2101	4.4111	-4.1764	-6.4804	4.2265	-8.6830	0.39375	0.24740	0.73160	85.596
13	-1.2101	4.4111	-4.1763	-6.4804	4.2264	-8.6829	0.39375	0.24740	0.73160	85.596
15	-1.2101	4.4111	-4.1763	-6.4804	4.2264	-8.6829	0.39375	0.24740	0.73160	85.596
Vel	-1.2101	4.4111	-4.1764	-6.4804	4.2264	-8.6829	0.3938		0.7316	

Table 4. Results for a single-layer Metal/Ceramic square plate with $a = b = 1 \text{ m}$, $a/h = 10$

I_1	$\bar{u}_1(0.5)$	$\bar{u}_3(0.5)$	$\bar{\sigma}_{11}(0.5)$	$\bar{\sigma}_{12}(0.5)$	$\bar{\sigma}_{13}(0.25)$	$\bar{\sigma}_{33}(0)$	$\bar{\Theta}(0)$	$\bar{q}_1(0)$	$\bar{q}_3(-0.5)$	$\bar{\eta}(0)$
3	-1.2095	3.6353	-3.0497	-6.4773	4.7296	-1259.0	0.42763	0.42763	0.71051	92.759
5	-1.2140	3.6416	-4.1605	-6.5015	5.3713	-13.790	0.42404	0.42404	0.80216	92.184
7	-1.2124	3.6337	-4.1555	-6.4928	4.4563	-9.7655	0.42401	0.42401	0.80723	92.176
9	-1.2124	3.6337	-4.1555	-6.4928	4.4699	-9.1531	0.42401	0.42401	0.80747	92.176
11	-1.2124	3.6337	-4.1555	-6.4928	4.4704	-9.1627	0.42401	0.42401	0.80748	92.176
13	-1.2124	3.6337	-4.1555	-6.4928	4.4703	-9.1622	0.42401	0.42401	0.80748	92.176
15	-1.2124	3.6337	-4.1555	-6.4928	4.4703	-9.1622	0.42401	0.42401	0.80748	92.176
Vel	-1.2124	3.6337	-4.1555	-6.4928	4.4703	-9.1622	0.4240		0.8075	

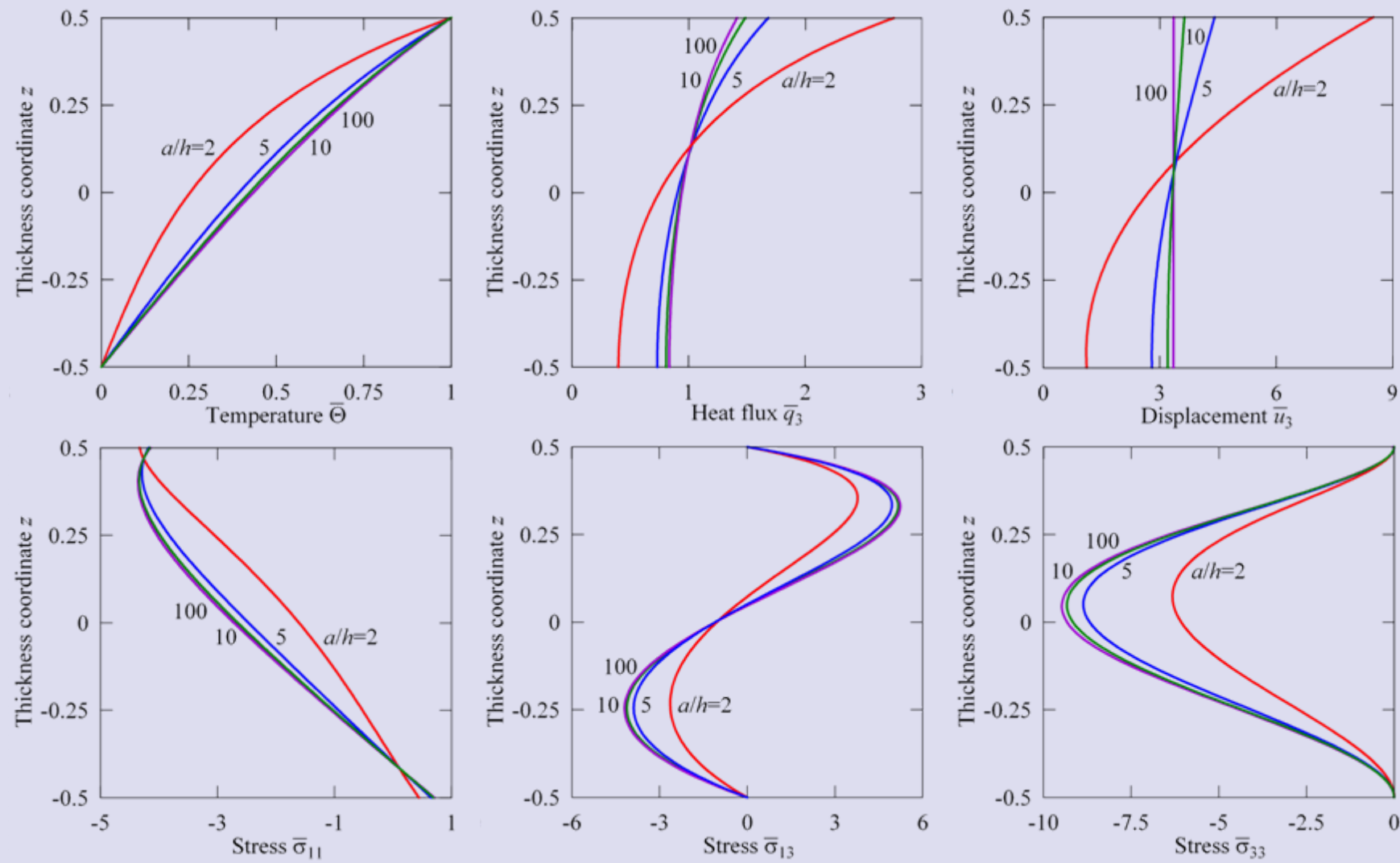
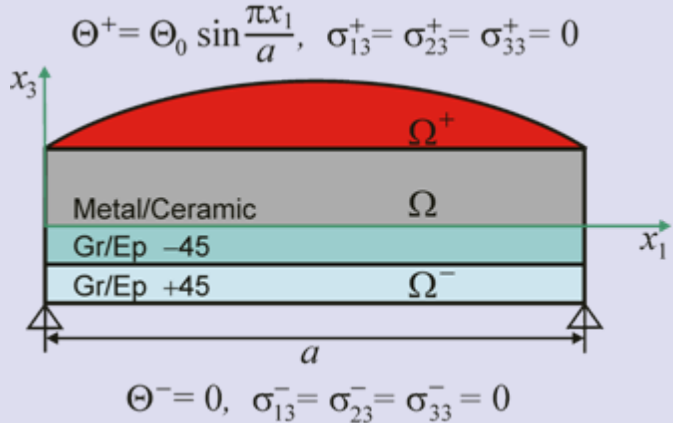


Figure 2. Through-thickness distributions of temperature, heat flux, transverse displacement and stresses of the single-layer Metal/Ceramic plate for $I_1 = 13$

3. Laminated FG Plate in Cylindrical Bending under Temperature Loading



Analytical solution

$$\Theta^{(n)i_n} = \sum_r \Theta_r^{(n)i_n} \sin \frac{r\pi x_1}{a}, \quad u_1^{(n)i_n} = \sum_r u_{1r}^{(n)i_n} \cos \frac{r\pi x_1}{a}$$

$$u_2^{(n)i_n} = \sum_r u_{2r}^{(n)i_n} \cos \frac{r\pi x_1}{a}, \quad u_3^{(n)i_n} = \sum_r u_{3r}^{(n)i_n} \sin \frac{r\pi x_1}{a}$$

Mori-Tanaka method is used for evaluating material properties of the Metal/Ceramic layer with

$E_m = 7 \times 10^{10} \text{ Pa}, \quad v_m = 0.3, \quad \alpha_m = 23.4 \times 10^{-6} \text{ 1/K}, \quad k_m = 233 \text{ W/mK}, \quad \rho_m = 2707 \text{ Kg/m}^3, \quad c_m = 896 \text{ J/KgK}$

$E_c = 4.27 \times 10^{11} \text{ Pa}, \quad v_c = 0.17, \quad \alpha_c = 4.3 \times 10^{-6} \text{ 1/K}, \quad k_c = 65 \text{ W/mK}, \quad \rho_c = 3100 \text{ Kg/m}^3, \quad c_c = 670 \text{ J/KgK}$

$V_m = 1 - V_c, \quad V_c = V_c^- + (V_c^+ - V_c^-)(2z)^\gamma, \quad z = x_3 / h, \quad V_c^- = 0, \quad V_c^+ = 0.5, \quad \gamma = 2, \quad T_0 = 293 \text{ K}$

where V_c^- , V_c^+ – volume fractions of the ceramic phase on bottom and top surfaces

Dimensionless variables in crucial points

$$\bar{\Theta} = \Theta(a/2, z)/\Theta_0, \quad \bar{q}_3 = -aq_3(a/2, z)/k_m\Theta_0, \quad \bar{\eta} = \eta(a/2, z)/E_m\alpha_m^2\Theta_0$$

$$\bar{u}_\alpha = 10u_\alpha(0, z)/a\alpha_m\Theta_0, \quad \bar{u}_3 = 100hu_3(a/2, z)/a^2\alpha_m\Theta_0$$

$$\bar{\sigma}_{11} = 10\sigma_{11}(a/2, z)/E_m\alpha_m\Theta_0, \quad \bar{\sigma}_{12} = 10\sigma_{12}(0, z)/E_m\alpha_m\Theta_0$$

$$\bar{\sigma}_{\alpha 3} = 100a\sigma_{\alpha 3}(0, z)/hE_m\alpha_m\Theta_0, \quad \bar{\sigma}_{33} = 100a^2\sigma_{33}(a/2, z)/h^2E_m\alpha_m\Theta_0$$

Table 5. Results for a three-layer FG plate in cylindrical bending with $a/h = 2$

I_n	$\bar{u}_1(0.5)$	$\bar{u}_3(0.5)$	$\bar{\sigma}_{11}(0.5)$	$\bar{\sigma}_{12}(0.5)$	$\bar{\sigma}_{13}(0)$	$\bar{\sigma}_{23}(0)$	$\bar{\sigma}_{33}(0)$	$\bar{\Theta}(-0.125)$	$\bar{q}_3(0)$	$\bar{\eta}(-0.125)$
5	-3.2361	16.213	8.1430	0.57593	-15.268 -15.585	6.0563 6.0669	-12.182 -9.2884	0.17634	0.33688 0.21846	25.797
7	-3.2330	16.191	8.1348	0.57574	-15.191 -15.183	6.0485 6.0481	-10.454 -10.374	0.17624	0.34081 0.33462	25.787
9	-3.2330	16.191	8.1359	0.57575	-15.189 -15.189	6.0482 6.0482	-10.420 -10.418	0.17624	0.34088 0.34058	25.787
11	-3.2330	16.191	8.1360	0.57575	-15.189 -15.189	6.0482 6.0482	-10.420 -10.420	0.17624	0.34088 0.34087	25.787
13	-3.2330	16.191	8.1360	0.57575	-15.189 -15.189	6.0482 6.0482	-10.420 -10.420	0.17624	0.34088 0.34088	25.787

Table 6. Results for a three-layer FG plate in cylindrical bending with $a/h = 10$

I_n	$\bar{u}_1(0.5)$	$\bar{u}_3(0.5)$	$\bar{\sigma}_{11}(0.5)$	$\bar{\sigma}_{12}(0.5)$	$\bar{\sigma}_{13}(0)$	$\bar{\sigma}_{23}(0)$	$\bar{\sigma}_{33}(0)$	$\bar{\Theta}(-0.125)$	$\bar{q}_3(0)$	$\bar{\eta}(-0.125)$
5	-3.6562	10.382	11.139	0.36661	-18.896 -19.640	3.4801 3.4897	-18.347 -10.309	0.67613	0.58345 0.55498	98.669
7	-3.6526	10.364	11.146	0.36569	-18.920 -18.905	3.4729 3.4728	-18.132 -16.795	0.67613	0.58347 0.58200	98.669
9	-3.6527	10.364	11.147	0.36569	-18.920 -18.920	3.4729 3.4729	-18.132 -18.054	0.67613	0.58347 0.58340	98.669
11	-3.6527	10.364	11.148	0.36569	-18.920 -18.920	3.4729 3.4729	-18.132 -18.129	0.67613	0.58347 0.58347	98.669
13	-3.6527	10.364	11.148	0.36569	-18.920 -18.920	3.4729 3.4729	-18.132 -18.132	0.67613	0.58347 0.58347	98.669

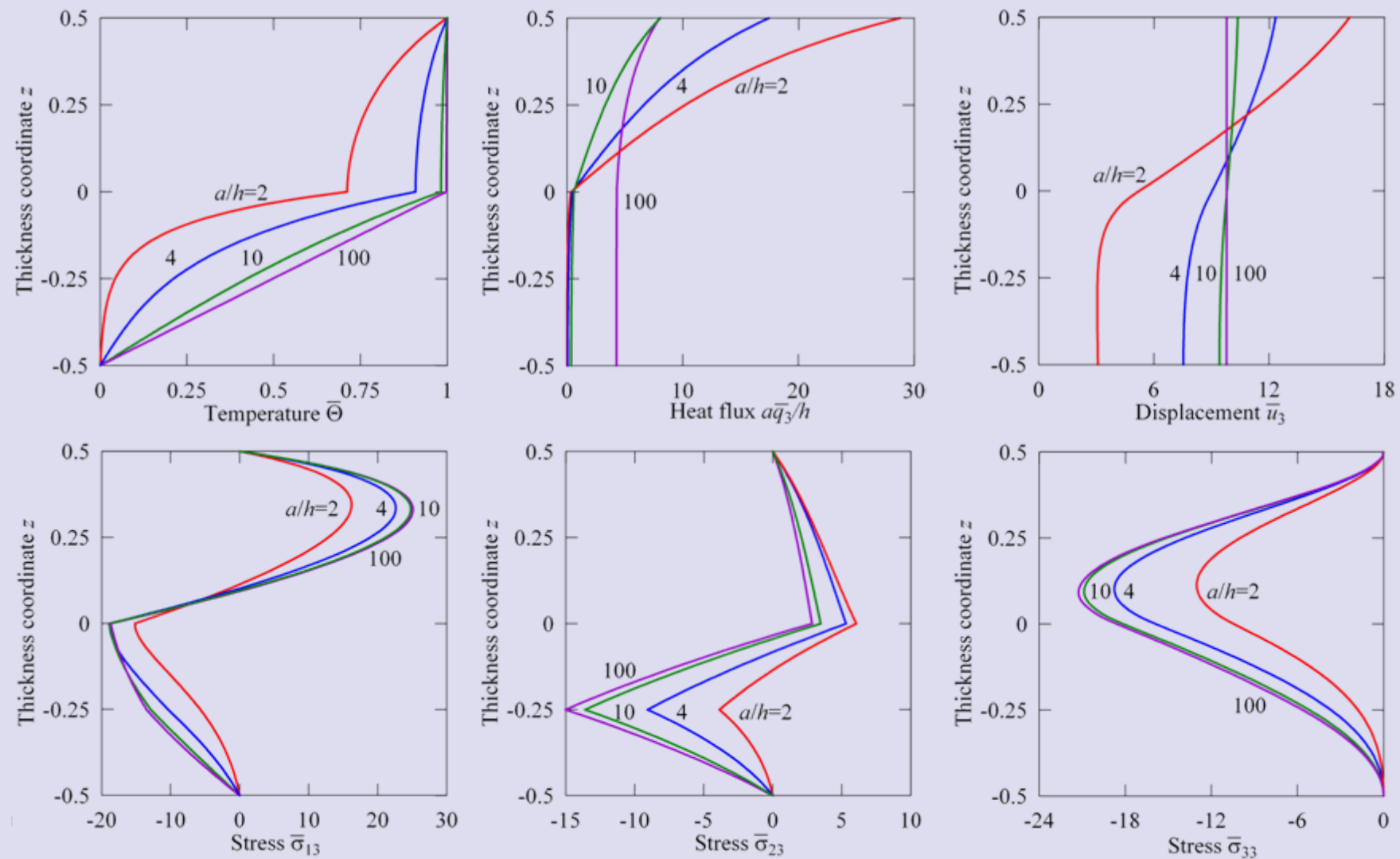
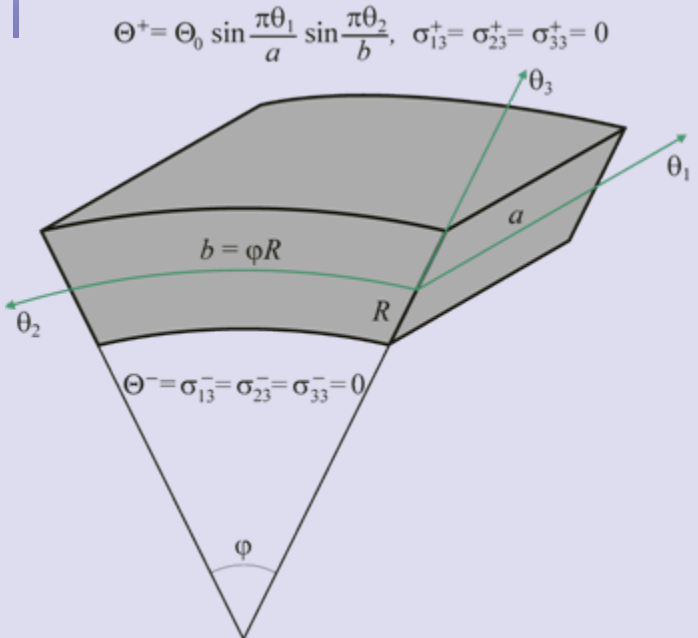


Figure 3. Through-thickness distributions of temperature, heat flux, transverse displacement and stresses of the three-layer plate for $I_1 = I_2 = I_3 = 13$

4. Two-Phase FG Cylindrical Shell under Temperature Loading



Analytical solution

$$\Theta^{(n)i_n} = \sum_{r,s} \Theta_{rs}^{(n)i_n} \sin \frac{r\pi X_1}{a} \sin \frac{s\pi X_2}{b}, \quad u_1^{(n)i_n} = \sum_{r,s} u_{1rs}^{(n)i_n} \cos \frac{r\pi X_1}{a} \sin \frac{s\pi X_2}{b}$$

$$u_2^{(n)i_n} = \sum_{r,s} u_{2rs}^{(n)i_n} \sin \frac{r\pi X_1}{a} \cos \frac{s\pi X_2}{b}, \quad u_3^{(n)i_n} = \sum_{r,s} u_{3rs}^{(n)i_n} \sin \frac{r\pi X_1}{a} \sin \frac{s\pi X_2}{b}$$

Mori-Tanaka method is used for evaluating material properties of the Metal/Ceramic shell

$$V_m = 1 - V_c, \quad V_c = V_c^- + (V_c^+ - V_c^-)(0.5 + z)^\gamma$$

$$z = x_3 / h, \quad V_c^- = 0, \quad V_c^+ = 0.5, \quad \gamma = 2$$

where V_c^- , V_c^+ – volume fractions of the ceramic phase on bottom and top surfaces

Dimensionless variables in crucial points

$$\bar{\Theta} = \Theta(a/2, b/2, z)/\Theta_0, \quad \bar{q}_3 = -hq_3(a/2, b/2, z)/k_m\Theta_0, \quad \bar{\eta} = \eta(a/2, b/2, z)/E_m\alpha_m^2\Theta_0$$

$$\bar{u}_1 = 10u_1(0, b/2, z)/R\alpha_m\Theta_0, \quad \bar{u}_2 = 10u_2(a/2, 0, z)/R\alpha_m\Theta_0, \quad \bar{u}_3 = 100hu_3(a/2, b/2, z)/R^2\alpha_m\Theta_0$$

$$\bar{\sigma}_{\alpha\alpha} = 10\sigma_{\alpha\alpha}(a/2, b/2, z)/E_m\alpha_m\Theta_0, \quad \bar{\sigma}_{12} = 10\sigma_{12}(0, 0, z)/E_m\alpha_m\Theta_0$$

$$\bar{\sigma}_{13} = 100R\sigma_{13}(0, b/2, z)/hE_m\alpha_m\Theta_0, \quad \bar{\sigma}_{23} = 100R\sigma_{23}(a/2, 0, z)/hE_m\alpha_m\Theta_0$$

$$\bar{\sigma}_{33} = 100R\sigma_{33}(a/2, b/2, z)/hE_m\alpha_m\Theta_0, \quad a = 4\text{m}, \quad b = \varphi R, \quad R = 1\text{m}, \quad \varphi = \pi/2, \quad T_0 = 293\text{K}$$

Table 7. Results for a single-layer Metal/Ceramic cylindrical shell with $a/h = 2$

I_1	$\bar{u}_1(0.5)$	$\bar{u}_2(0.5)$	$\bar{u}_3(0.5)$	$\bar{\sigma}_{11}(0.5)$	$\bar{\sigma}_{22}(0.5)$	$\bar{\sigma}_{12}(0.5)$	$\bar{\sigma}_{13}(0)$	$\bar{\sigma}_{23}(0)$	$\bar{\sigma}_{33}(0)$	$\bar{\Theta}(0)$	$\bar{q}_3(-0.5)$	$\bar{\eta}(0)$
3	-2.5424	-1.5393	30.845	-5.3359	3.8713	-4.4975	0.56580	5.9348	-25.316	0.43434	0.73737	94.251
5	-2.5397	-1.5852	30.872	-6.1923	3.1512	-4.5245	1.5326	11.283	-4.0027	0.43435	0.90909	94.431
7	-2.5355	-1.5843	30.806	-6.1897	3.1388	-4.5183	1.3799	11.256	-4.0410	0.43461	0.91050	94.484
9	-2.5355	-1.5844	30.806	-6.1890	3.1395	-4.5183	1.3638	11.259	-4.0376	0.43463	0.91186	94.490
11	-2.5355	-1.5843	30.806	-6.1891	3.1395	-4.5183	1.3676	11.263	-4.0390	0.43463	0.91199	94.490
13	-2.5355	-1.5843	30.806	-6.1892	3.1394	-4.5183	1.3667	11.262	-4.0389	0.43463	0.91202	94.490
15	-2.5355	-1.5843	30.806	-6.1892	3.1393	-4.5183	1.3670	11.263	-4.0387	0.43463	0.91203	94.490
17	-2.5355	-1.5843	30.806	-6.1892	3.1393	-4.5183	1.3669	11.263	-4.0387	0.43463	0.91203	94.490

Table 8. Results for a single-layer Metal/Ceramic cylindrical shell with $a/h = 10$

I_1	$\bar{u}_1(0.5)$	$\bar{u}_2(0.5)$	$\bar{u}_3(0.5)$	$\bar{\sigma}_{11}(0.5)$	$\bar{\sigma}_{22}(0.5)$	$\bar{\sigma}_{12}(0.5)$	$\bar{\sigma}_{13}(0)$	$\bar{\sigma}_{23}(0)$	$\bar{\sigma}_{33}(0)$	$\bar{\Theta}(0)$	$\bar{q}_3(-0.5)$	$\bar{\eta}(0)$
3	-5.1888	8.7907	24.985	-0.54135	4.5306	-2.5392	1.1008	2.3140	-133.41	0.44789	0.79156	97.474
5	-5.1689	8.6992	24.828	-1.7182	3.4238	-2.5682	3.1211	7.2866	-3.5090	0.44497	0.87090	97.050
7	-5.1658	8.6957	24.815	-1.6988	3.4379	-2.5656	3.1471	7.3990	-2.3474	0.44492	0.87511	97.042
9	-5.1658	8.6956	24.815	-1.6987	3.4380	-2.5656	3.1452	7.3997	-2.2913	0.44492	0.87532	97.043
11	-5.1658	8.6956	24.815	-1.6987	3.4380	-2.5656	3.1455	7.4002	-2.2919	0.44492	0.87533	97.043
13	-5.1658	8.6956	24.815	-1.6987	3.4380	-2.5656	3.1454	7.4001	-2.2918	0.44492	0.87533	97.043
15	-5.1658	8.6956	24.815	-1.6987	3.4380	-2.5656	3.1455	7.4001	-2.2918	0.44492	0.87533	97.043

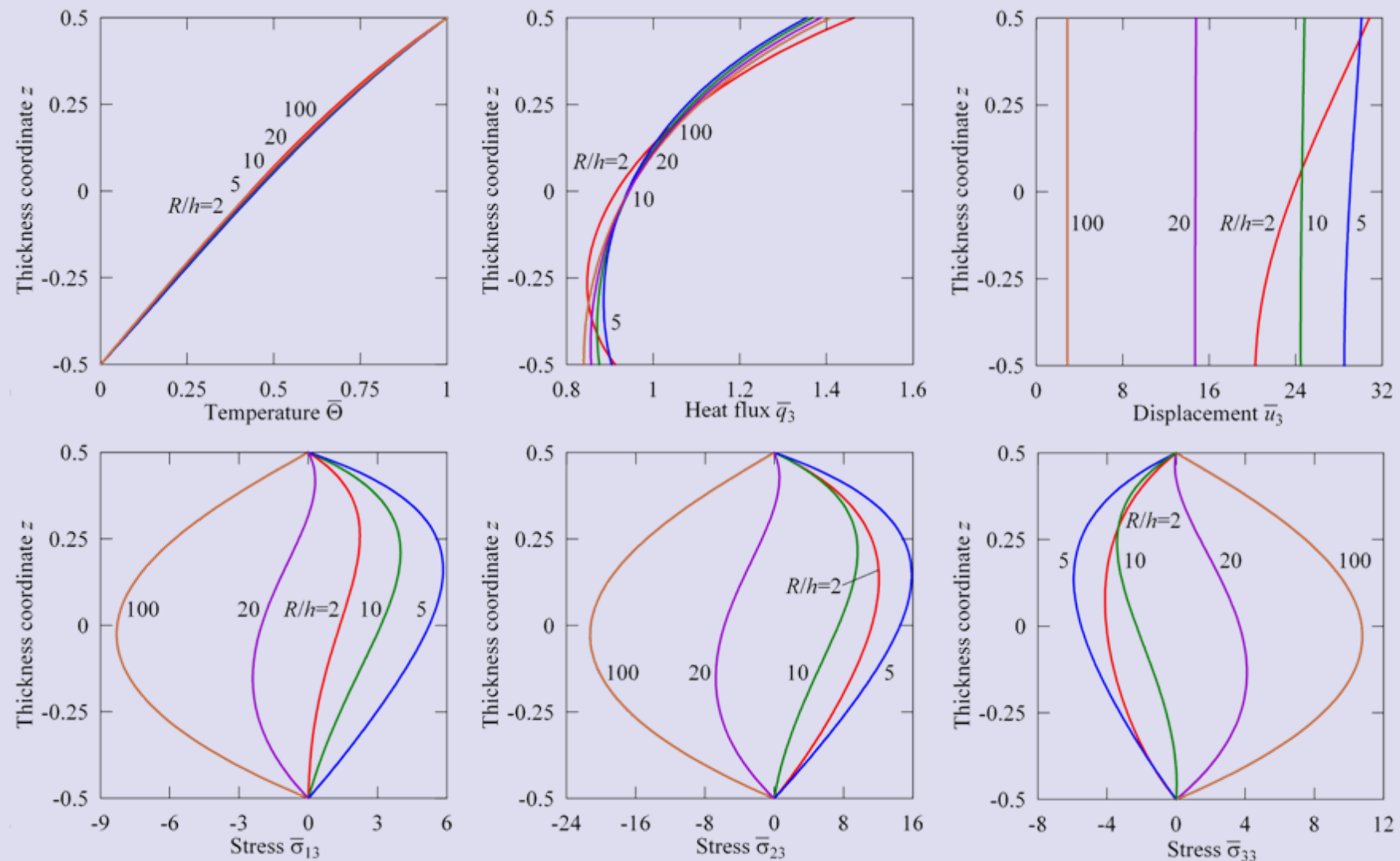
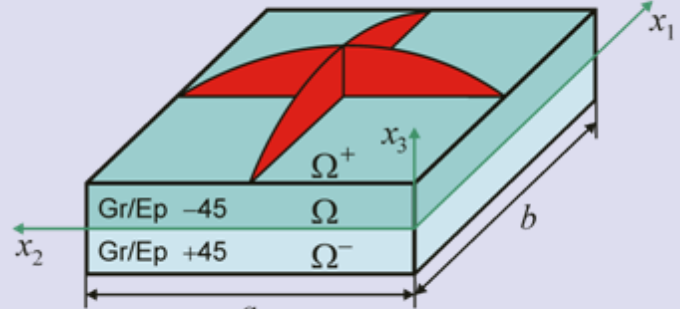


Figure 4. Through-thickness distributions of temperature, heat flux, transverse displacement and stresses of the single-layer Metal/Ceramic cylindrical shell for $l_1 = 13$

5. Antisymmetric Angle-Ply Rectangular Plate under Temperature Loading

$$\Theta^+ = -\Theta_0 \sin \frac{r\pi x_1}{a} \sin \frac{s\pi x_2}{b}, \quad \sigma_{13}^+ = \sigma_{23}^+ = \sigma_{33}^+ = 0$$



$$\Theta^- = \Theta_0 \sin \frac{r\pi x_1}{a} \sin \frac{s\pi x_2}{b}, \quad \sigma_{13}^- = \sigma_{23}^- = \sigma_{33}^- = 0$$

Analytical solution ($r = s = 1$)

$$\begin{aligned}\Theta^{(n)i_n} &= \bar{\Theta}_0^{(n)i_n} \sin \frac{r\pi x_1}{a} \sin \frac{s\pi x_2}{b} + \tilde{\Theta}_0^{(n)i_n} \cos \frac{r\pi x_1}{a} \cos \frac{s\pi x_2}{b} \\ u_1^{(n)i_n} &= \bar{u}_{10}^{(n)i_n} \cos \frac{r\pi x_1}{a} \sin \frac{s\pi x_2}{b} + \tilde{u}_{10}^{(n)i_n} \sin \frac{r\pi x_1}{a} \cos \frac{s\pi x_2}{b} \\ u_2^{(n)i_n} &= \bar{u}_{20}^{(n)i_n} \sin \frac{r\pi x_1}{a} \cos \frac{s\pi x_2}{b} + \tilde{u}_{20}^{(n)i_n} \cos \frac{r\pi x_1}{a} \sin \frac{s\pi x_2}{b} \\ u_3^{(n)i_n} &= \bar{u}_{30}^{(n)i_n} \sin \frac{r\pi x_1}{a} \sin \frac{s\pi x_2}{b} + \tilde{u}_{30}^{(n)i_n} \cos \frac{r\pi x_1}{a} \cos \frac{s\pi x_2}{b}\end{aligned}$$

Dimensionless variables in crucial points

$$\bar{u}_1 = u_1(0, a/2, z) / a\alpha_r\Theta_0, \quad \bar{u}_3 = u_3(a/2, a/2, z) / a\alpha_r\Theta_0, \quad \bar{\sigma}_{11} = \sigma_{11}(a/2, a/2, z) / E_r\alpha_r\Theta_0$$

$$\bar{\sigma}_{12} = \sigma_{12}(0, 0, z) / E_r\alpha_r\Theta_0, \quad \bar{\sigma}_{13} = \sigma_{13}(0, a/2, z) / E_r\alpha_r\Theta_0, \quad \tilde{\sigma}_{13} = \sigma_{13}(a/2, 0, z) / E_r\alpha_r\Theta_0$$

$$\bar{\sigma}_{33} = \sigma_{33}(a/2, a/2, z) / E_r\alpha_r\Theta_0, \quad \tilde{\sigma}_{33} = \sigma_{33}(0, 0, z) / E_r\alpha_r\Theta_0, \quad \bar{\eta} = \eta(a/2, a/2, z) / E_r\alpha_r^2\Theta_0$$

$$\bar{\Theta} = \Theta(a/2, a/2, z) / \Theta_0, \quad \tilde{\Theta} = \Theta(0, 0, z) / \Theta_0, \quad \bar{q}_3 = aq_3(a/2, a/2, z) / k_r\Theta_0, \quad z = x_3 / h$$

$$E_r = 10^9 \text{ Pa}, \quad \alpha_r = 10^{-6} \text{ 1/K}, \quad k_r = 1 \text{ W/mK}$$

Table 9. Results for the antisymmetric angle-ply square plate with $a = b = 1\text{ m}$ and $a/h = 4$

I_n	$\bar{u}_1(0.5)$	$\bar{u}_3(0)$	$\bar{\sigma}_{11}(-0.5)$	$\bar{\sigma}_{12}(0.5)$	$\bar{\sigma}_{13}(0.25)$	$\tilde{\sigma}_{13}(0.25)$	$\bar{\sigma}_{33}(0.25)$	$\tilde{\sigma}_{33}(0.25)$	$\bar{\Theta}(0.25)$	$\tilde{\Theta}(0.25)$	$\bar{q}_3(0.25)$
3	2.0154	-3.5218	54.229	112.53	3.8370	22.629	46.852	35.104	-0.26185	0.23471	4.0000
5	2.2910	-4.1102	127.59	151.80	-8.0048	34.303	8.7527	14.509	-0.30086	0.24531	2.2963
7	2.2949	-4.1179	132.69	152.24	-6.9499	33.219	3.2107	8.9775	-0.30022	0.24674	2.5068
9	2.2949	-4.1179	133.01	152.23	-7.0044	33.273	3.5188	9.2855	-0.30025	0.24670	2.4935
11	2.2949	-4.1179	133.02	152.23	-7.0028	33.272	3.5090	9.2757	-0.30025	0.24671	2.4939
13	2.2949	-4.1179	133.02	152.23	-7.0028	33.272	3.5092	9.2759	-0.30025	0.24671	2.4939

Table 10. Results for the antisymmetric angle-ply square plate with $a = b = 1\text{ m}$ and $a/h = 10$

I_n	$\bar{u}_1(0.5)$	$\bar{u}_3(0)$	$\bar{\sigma}_{11}(-0.5)$	$\bar{\sigma}_{12}(0.5)$	$\bar{\sigma}_{13}(0.25)$	$\tilde{\sigma}_{13}(0.25)$	$\bar{\sigma}_{33}(0.25)$	$\tilde{\sigma}_{33}(0.25)$	$\bar{\Theta}(0.25)$	$\tilde{\Theta}(0.25)$	$\bar{q}_3(0.25)$
3	1.5132	-8.6313	118.13	160.54	1.5982	13.358	18.017	15.449	-0.40974	0.15819	10.000
5	1.5709	-8.9944	141.82	170.57	-5.3058	20.934	1.3139	2.6692	-0.41234	0.16073	8.9303
7	1.5710	-8.9945	142.23	170.56	-5.1795	20.807	0.86386	2.2198	-0.41233	0.16075	8.9569
9	1.5710	-8.9945	142.23	170.56	-5.1806	20.808	0.86837	2.2243	-0.41233	0.16075	8.9566
11	1.5710	-8.9945	142.23	170.56	-5.1806	20.808	0.86835	2.2243	-0.41233	0.16075	8.9566

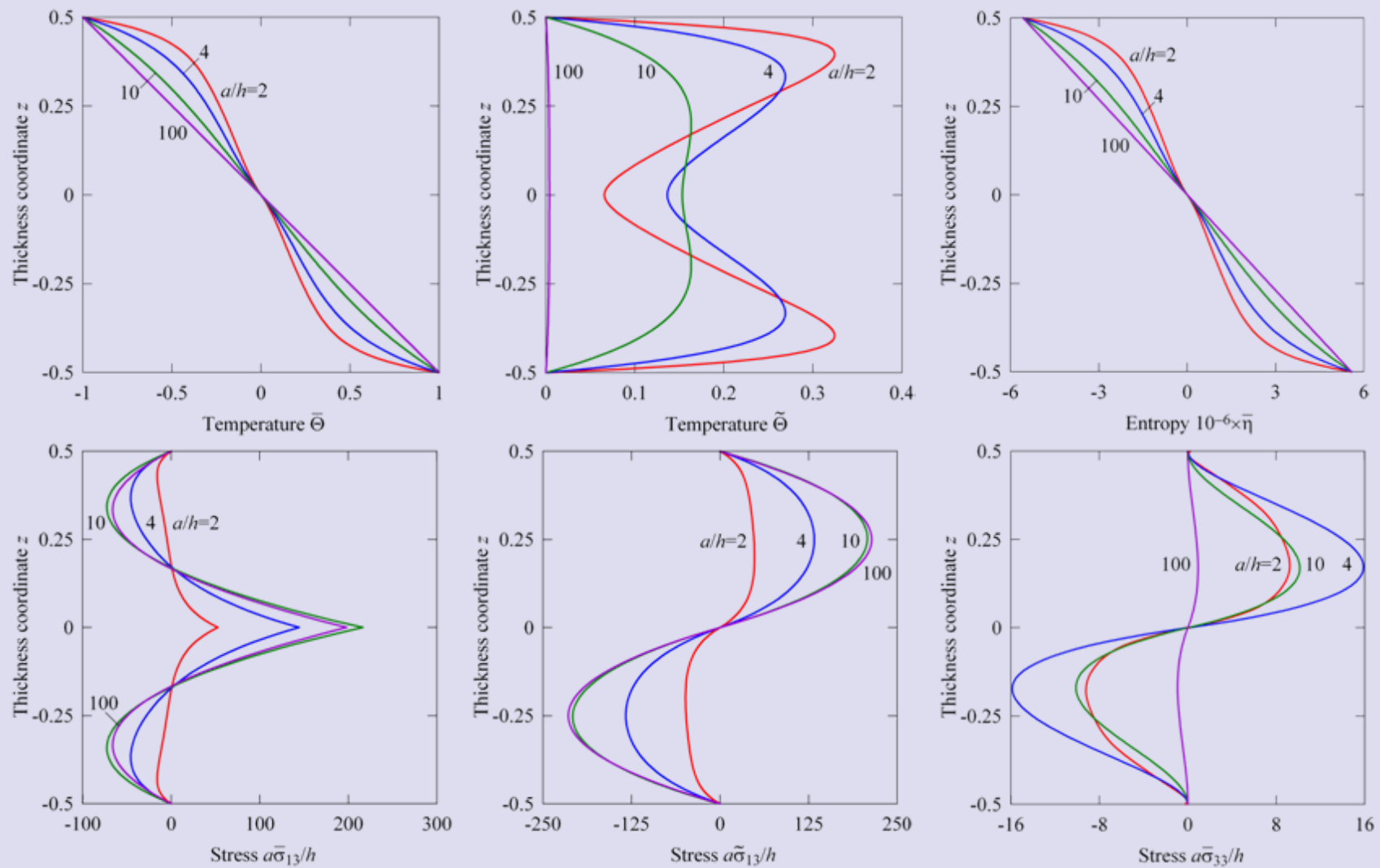


Figure 5. Through-thickness distributions of symmetric and unsymmetric components of temperature, entropy and transverse stresses of the antisymmetric angle-ply square plate for $I_1 = I_2 = 11$

Thanks for your attention!